

ROLLING NOISE REDUCTION THROUGH GA-BASED WHEEL SHAPE OPTIMIZATION TECHNIQUES

X. Garcia-Andrés*, J. Gutiérrez-Gil, V. T. Andrés, J. Martínez-Casas and
F. D. Denia

Instituto Universitario de Ingeniería Mecánica y Biomecánica (I2MB)
Universidad Politècnica de València
Valencia, Spain

e-mail: xagaran@upv.es*, jorgugil@upv.es, vicanrui@etsid.upv.es, jomarc12@mcm.upv.es,
fdenia@mcm.upv.es

Key words: Railway wheel, Geometric optimization, Genetic Algorithms, Rolling noise

Abstract: *Railway rolling noise is nowadays a major source of acoustic pollution in urban areas, with nearly up to 12 million people daily affected in Europe by this phenomenon. Hence, the search for ways of decreasing such noise radiation has become a highly active and significant research field. Following this approach, a Genetic Algorithms-based shape optimization of the railway wheel is developed with the aim of minimizing rolling noise. Different approaches are considered to address the problem, such as directly minimizing radiated Sound poWer Level (SWL) or using the maximization of the natural frequencies if computational efficiency is especially critical. A parametric Finite Element model is implemented for the wheel based on the most relevant geometric parameters in rolling noise radiation. For the acoustic calculation, the sound radiation models used in the TWINS software are adopted, which also accounts for the whole dynamics of the wheel/rail system. Furthermore, for every candidate wheel proposed, a structural analysis is computed in order to check design feasibility in accordance with the corresponding standard. In all cases, new geometries for the wheel cross section are achieved that reduce the radiated rolling noise.*

1 INTRODUCTION

Railways are a highly efficient, cost-effective and low polluting transportation system. Unfortunately, there are also some drawbacks that need to be handled if the rail network is to be further expanded. Such issues are mainly related to acoustic pollution, what becomes especially important along urban environments, where it is estimated that about 12 million people are affected daily in Europe by the sound emitted by railway vehicles [1].

In that sense, one of the predominant types of noise emitted by railway vehicles is rolling noise [2], generated by the vibration of the wheel and track caused by the interaction force that emerges as a result of the irregularities present in their surfaces [3]. Through the different range of possible approaches that can be followed for rolling noise mitigation, those that consider its control at source are acknowledged as considerable cost-effective measures [4].

The present work therefore presents a procedure for the reduction of railway rolling noise by achieving optimal wheel geometries that minimize sound radiation. This is done by means of the global optimization technique known as Genetic Algorithm (GA) using two different methodologies, a first one based on the computed Sound Power Level (SWL), what includes solving the whole dynamic interaction, and another focused on the modal properties of the wheel. Moreover, the structural feasibility of each proposed candidate during the search is assured.

The document is structured as follows: firstly, the theoretical model used for the dynamic and acoustic calculations is introduced; Secondly, the optimization procedure is described along

with the defined objective functions and wheel shape parametrization; and, later, the results obtained are shown. Finally, a concluding discussion is presented.

2 THEORETICAL MODEL

For the present work, a methodology based on that of the commercial software TWINS is developed [5]. A system composed by a wheel and a continuously supported rail interacting at a contact point is considered. In order to derive the rolling noise radiation produced by the wheel, the whole coupled dynamic response of each of the components involved in the wheel/track interaction is solved through the use of linearised models in the frequency domain. Then, the wheel sound power is obtained with a semi-analytical formulation capable of computing the wheel acoustic efficiencies from the dynamic behaviour of its cross-section geometry.

2.1 Wheel response

The wheel response for the j th degree of freedom (d.o.f) is given by

$$u_{w,j} = - \sum_{i=1}^3 H_{w,ji} F_{c,i}, \quad (1)$$

where $H_{w,ji}$ is the receptance of the wheel for the j th d.o.f. when the force is applied at the contact point in the i th direction and $F_{c,i}$ is the value of the contact force in the i th direction; x , y and z being represented by directions 1, 2 and 3, respectively.

The receptance of the wheel is given by modal superposition, with the associated modeshapes classified according to its number of nodal diameters n and nodal circumferences m , as [6]

$$H_{w,jk}(\omega) = \sum_{n=0}^{\infty} \sum_{m=0}^{\infty} \frac{\Psi_{nm,j} \Psi_{nm,k}}{m_{nm}(\omega_{nm}^2 - \omega^2 + 2i\xi_{nm}\omega_{nm}\omega)}, \quad (2)$$

where, $\Psi_{nm,j}$ and $\Psi_{nm,k}$ are the modal amplitudes of the modeshape (n, m) for direction j and k , respectively, m_{nm} is the modal mass of the corresponding modeshape, ω_{nm} its natural frequency, ξ_{nm} the modal damping ratio and ω the angular frequency considered.

Regarding the derivation of the contact force \bar{F}_c , assuming that the excitation of the system is produced by the presence of a roughness amplitude r acting in the vertical direction, it can be stated that

$$\bar{r} = \mathbf{H}_{sys} \bar{F}_c, \quad (3)$$

with \bar{r} being a vector with amplitude r in the vertical direction and \mathbf{H}_{sys} the combined receptance of each component of the system defined as [2]

$$\mathbf{H}_{sys} = \mathbf{H}_w + \mathbf{H}_r + \mathbf{H}_c, \quad (4)$$

where \mathbf{H}_w , \mathbf{H}_r and \mathbf{H}_c are the receptances in matrix form of the wheel, rail and contact, respectively. In the present model, the rail receptance \mathbf{H}_r is characterized considering the rail as a Timoshenko beam on a continuous foundation [2] and the contact receptance \mathbf{H}_c describes the wheel/track interaction by means of a contact spring [7].

2.2 Wheel sound power

As a means to compute the radiated sound power of the wheel, the surface of this component is divided into six concentric rings and the tyre surface. Then, their velocity responses are calculated with the dynamic model introduced in the previous section and used for the

computation of the corresponding sound radiation. Therefore, it is possible to derive the wheel sound power W through [2]

$$W = \rho c_0 \sum_l^{N_m} \left(\sigma_l^a \sum_j (S_{a,j} \langle \tilde{v}_{a,jl}^2 \rangle) + \sigma_l^r S_r \langle \tilde{v}_{r,l}^2 \rangle \right), \quad (5)$$

where index l refers to each the N_m modeshapes considered, ρ is the air density, c_0 the speed of sound, $\langle \tilde{v}_{a,jl}^2 \rangle$ and $\langle \tilde{v}_{r,l}^2 \rangle$ represent the mean squared vibration velocity averaged over time and surface area of the ring j and l^{th} modeshape for the axial and radial directions, respectively; $S_{a,j}$ refers to the axial area of the j^{th} ring, S_r to the surface used for the radial radiation and σ_l^a and σ_l^r are the radiation efficiencies of the axial and radial contribution, respectively, for the l^{th} mode.

The radiation efficiencies, which are defined as the ratio of the amount of acoustic power radiated compared to that of a piston of the same area on an infinite wall when vibrating in the same manner [8], are obtained with a semi-analytical formulation detailed in [9].

3 OPTIMIZATION PROCEDURE

With the intention of minimizing the rolling noise radiated by the railway wheel, a Genetic Algorithms-based shape optimization procedure is developed and two different objective functions are studied: one based on the direct minimization of the radiated sound power ($L_{A,W}$ -min), and another focused on the maximization of the natural frequencies of the wheel (NF-max).

Additionally, for the purpose of establishing a way of generating the different geometries propose for testing by the GA, a parametric FE model is defined using general axisymmetric elements [10]. The wheel cross section is set by the geometric characteristics found to be the most influential for the acoustic radiation [9, 11]: wheel radius x_1 , fillet radius x_2 , web thickness x_3 and web offset x_4 . An overview of the described framework is presented in Fig. 1, while the design boundaries specified for this research are shown in Table 1. It should be noted that, as x_1 , x_2 and x_4 are absolute parameters whose value directly correspond to the corresponding geometric property, x_3 is defined as a proportionality factor of the reference thickness along the web. Besides, due to constraints in the design process related with the modification of the wheel radius, two different optimizations are run for each procedure: one considering all the components in the parametrization and another in which the radius is kept as constant with value $x_1 = 0.45$ m.

The optimization algorithm proceeds as follows: the first step is to create a set of wheel candidates by using the defined parametrization, which conforms the generation \mathbf{X}_i ; then, for every candidate \bar{x}_j in \mathbf{X}_i , the structural feasibility of each proposed wheel is checked by following the standard EN13979-1 [12]. If the candidate is feasible, a modal analysis to obtain the N_m modeshapes Ψ_{nm} and natural frequencies ω_{nm} , needed for the calculation of the studied objective functions, is carried out by the FEM software ANSYS APDL. Afterwards, modeshapes are identified and classified in accordance to the number of nodal diameters and nodal circumferences (n, m) they present and the selected objective function Obj is evaluated.

Table 1: Design domain for the optimization methodologies.

	x_1 [m]	x_2 [m]	x_3	x_4 [m]
Reference	0.45	0.0427	0.0681	0.0300
Lower Boundary	0.40	0.0364	-0.1000	-0.2700
Upper Boundary	0.50	0.0484	0.1000	0.2700

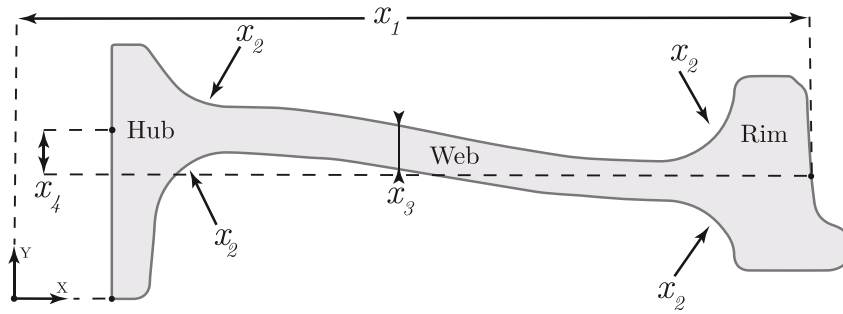


Figure 1: Design variables of the wheel cross section parametrization.

Once Obj has been computed for the whole generation, the stopping criteria is checked. If it is fulfilled, the candidate most suited for the objective function \bar{x}^* is selected as the Best Found Solution (BFS). Otherwise, a new generation is set that accounts for the geometrical information of the cross sections already analysed during each iteration and the described process is repeated. For further clarification, a flow diagram of the optimization algorithm is represented in Fig. 2.

3.1 Objective functions

As already mentioned in the previous sections, two different objective functions are used along the optimization algorithm, $L_{A,W}$ -min and NF-max. Below, their main features are explained with further detail.

3.1.1 $L_{A,W}$ -min methodology

In the $L_{A,W}$ -min methodology the goal is to directly minimize the radiated noise emitted by the wheel. With this intention, the SWL expressed in dB(A) is used, computed for every design as

$$SWL = 10 \log_{10} \left(\frac{W}{W_{ref}} \right) + A_{filter}, \quad (6)$$

where W is the sound power, $W_{ref} = 10^{-12}$ W and A_{filter} is the A-weighting filter for dB.

Next, Obj is defined as the summation in energy of the SWL in each frequency band.

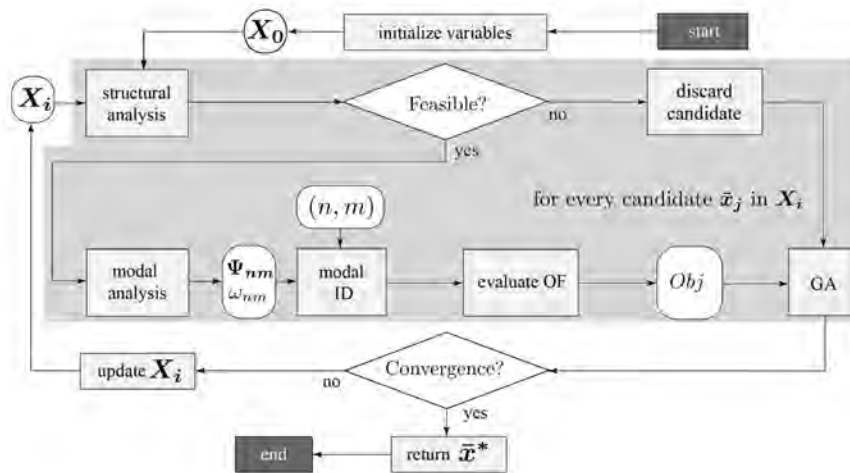


Figure 2: Flow diagram describing the optimization procedure.

Therefore,

$$Obj_{L_{A,W}} = 10 \log_{10} \left(\sum_{i=1}^{n_{cf}} 10^{\frac{SWL_i}{10}} \right), \quad (7)$$

where SWL_i is the SWL of the i th one-third octave band and n_{cf} the number of bands in the chosen frequency region.

3.1.2 NF-max methodology

In the NF-max methodology, the minimization of rolling noise is intended indirectly through the maximization of the natural frequencies of the wheel. The assumption made in this case is that, as the excitation of the system is dependent on the wheel-rail combined roughness and its content is lower in the high frequency region, shifting the natural frequencies to higher frequency regions should lead to wheel shapes whose vibration modes are less excited and, consequently, quieter designs. With this aim, the objective function Obj for the current methodology its defined as

$$Obj_{NF} = \frac{1}{\hat{\omega}_m}, \quad (8)$$

where $\hat{\omega}_m$ is the mean of all the N_m extracted natural frequencies of the wheel.

4 RESULTS

For the results presented in this section, the following specifications are used: an UIC54 rail with concrete bibloc sleepers separated 0.6 m, the parameters of which are shown in Table 2, and a standard roughness defined for a train speed of $V = 80$ km/h when a contact filter is applied [13]. In the dynamic calculations, the frequency range varies from 50 to 5000 Hz with a resolution of 1 Hz and the reference wheel, taken as a guideline to compare the changes observed for the wheel designs, is based on a simplified monobloc wheel with typical dimensions. As for the modal analysis made, a rigid constraint is applied at the nodes on the inner surface of the wheel hub, the maximum element size defined for the FE mesh is $h = 0.007$ m and a number of $N_m = 48$ modeshapes are considered. Additionally, in order to assure the correct development of the theoretical model, the combined SWL for all the components involved in the rolling noise radiation is compared to the results offered for the same case by the commercial package TWINS [5]. As it can be seen in Fig. 3, no significant discrepancies are observed, with a total variation in terms of energy of $\Delta L_{A,T} = 0.17$ dB(A).

The main results for both methodologies are presented in Table 3 and the wheel cross section geometries obtained for each procedure are shown in Fig. 4. The two approaches show a reduction in both the wheel SWL and total SWL for either the fixed radius case or the optimization with all the parameters. Thus, in the fixed radius case, it is clear that the obtained $L_{A,W}$ are lower than the reference wheel, with variations of $\Delta L_{A,W} = -3.94$ dB(A) and

Table 2: Track parameters used in SWL calculations.

Rail UIC54	Vertical	Lateral	Foundation	Vertical	Lateral
Bending stiffness EI [Nm ²]	$4.93 \cdot 10^6$	$0.87 \cdot 10^6$	Pad stiffness k'_p [N/m ²]	$2.17 \cdot 10^9$	$1.17 \cdot 10^8$
Shear coefficient κ	0.4	0.4	Pad loss factor η_p	0.25	0.25
Loss factor η_r	0.02	0.02	Ballast stiffness k'_b [N/m ²]	$1.17 \cdot 10^8$	$5.83 \cdot 10^7$
Mass per length ρA [kg/m]		54	Ballast loss factor η_b	2	2
Cross receptance level		-15	Sleeper mass per length m'_s [kg/m]	203.33	

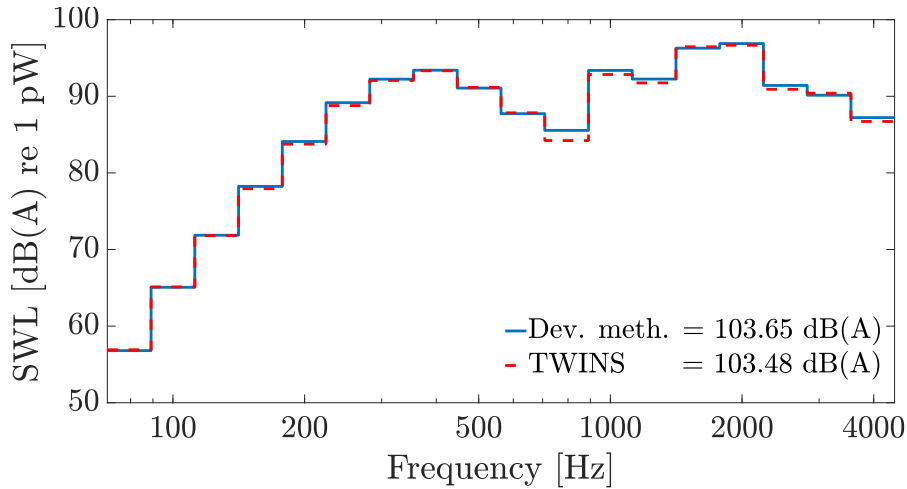


Figure 3: Total SWL produced by the commercial program TWINS (---) and the methodology developed in the present work (—)

$\Delta L_{A,W} = -1.11$ dB(A) for the $L_{A,W}$ -min and NF-max methodologies, respectively. Regarding the noise when considering all the components involved, reductions are kept with a change in $L_{A,T}$ of $\Delta L_{A,T} = -1.87$ dB(A) for $L_{A,W}$ -min and $\Delta L_{A,T} = -0.43$ dB(A) NF-max. When all the geometric parameters are considered in the optimization, quieter wheel designs are achieved with improvements of up to $\Delta L_{A,W} = -4.96$ dB(A) and $\Delta L_{A,T} = -2.05$ dB(A) for the $L_{A,W}$ -min approach. In all cases, an increase of the mean of the natural frequencies $\hat{\omega}_m$ is produced and the NF-max approach appears as computationally demanding methodology, requiring a lower number of generations n_{gen} to achieve convergence with a $\Delta n_{gen} = -24$ generations when compared with $L_{A,W}$ -min in the optimization with fixed radius.

Concerning the evolution of the wheel shape along the optimization procedures, different Response Surfaces (RS) are generated in order to study it. For each RS, a pair of the defined geometric parameters are chosen and evaluated for each objective function in 676 different points along the solution space, allocated in the form of a 26×26 evenly distributed sampling grid. Some of the most relevant RSs generated are represented in Fig. 5. As exemplified in the results shown in Fig. 5a, the objective function defined for the NF-max approach presents mainly a planar form and the greatest maximization of natural frequencies is related with the decrease of radius x_1 . Conversely, in the $L_{A,W}$ -min methodology, the observed behaviour is in a more complex and variable manner. This can be seen in Fig. 5b, which also reveal the predominance of the web offset x_4 variable, followed by the radius x_1 , in setting the value of the corresponding objective function. It should be noted that in all cases the minimum value obtained for the selected objective function were worse than that offered by the optimization.

Finally, for the purpose of further exploring the relation between Obj_{NF} and $Obj_{L_{A,W}}$, the

Table 3: BFS values for the optimization procedures. x_1 , x_2 and x_4 are expressed in m. All L_A values are expressed in dB(A).

Methodology	x_1	x_2	x_3	x_4	$L_{A,W}$	$\Delta L_{A,W}$	$L_{A,T}$	$\Delta L_{A,T}$
$L_{A,W}$-min (Fixed rad.)	0.4500	0.0484	0.1000	-0.0128	97.35	-3.94	102.28	-1.87
NF-max (Fixed rad.)	0.4500	0.0484	0.1000	-0.0270	100.18	-1.11	103.73	-0.43
$L_{A,W}$-min (All param.)	0.4222	0.0483	0.0999	-0.0102	96.33	-4.96	102.10	-2.05
NF-max (All param.)	0.4000	0.0484	0.1000	-0.0167	99.26	-2.03	103.10	-1.05
Ref.	0.4500	0.0427	0.0700	0.0300	101.29	-	104.16	-



Figure 4: Wheel shapes comparison for the BFSs obtained by the optimization procedure with the fixed radius case (left) and considering all the geometric parameters (right). In both cases the results are shown for the NF-max (orange) and $L_{A,W}$ -min (green) approaches together with the reference wheel (black).

objective function value $L_{A,W}$ for all candidates designs evaluated in the optimization runs is plotted against their natural frequencies mean in Fig. 6. Although some correlations can be found locally, there are not for the totality of sampled candidates: for the optimization with all the geometric parameters, the decreases of both objective functions value are coupled in the region where x_1 is above the optimum value ($x_1 = 0.42$ m), but below this point the trend shifts; and in the fixed radius case, a wide range of emitted noise is present for the candidates with minimum Obj_{NF} value. In both cases, the observable patterns are consistent with the existence of design variables with high influence on the acoustic behaviour but low on the fixing of the natural frequencies, as the web offset x_4 .

5 CONCLUSIONS

With the goal of reducing acoustic radiation, a geometric optimization of the railway wheel cross-section shape is performed by means of a GA-based optimizer. Two different methodologies are applied: the NF-max methodology, focused on the maximization of the natural frequencies, and the $L_{A,W}$ -min methodology, based on the direct minimization of the wheel SWL. Furthermore, response surfaces for different combinations of geometric parameters are carried out in order to study their behaviour along the optimization process.

Results reflect that in all approaches a reduction is accomplished for both the wheel SWL, with improvements of up to 4.96 dB(A) in the $L_{A,W}$ -min case, and the SWL when all components involved in the rolling noise radiation are considered. The differences in the evolution of

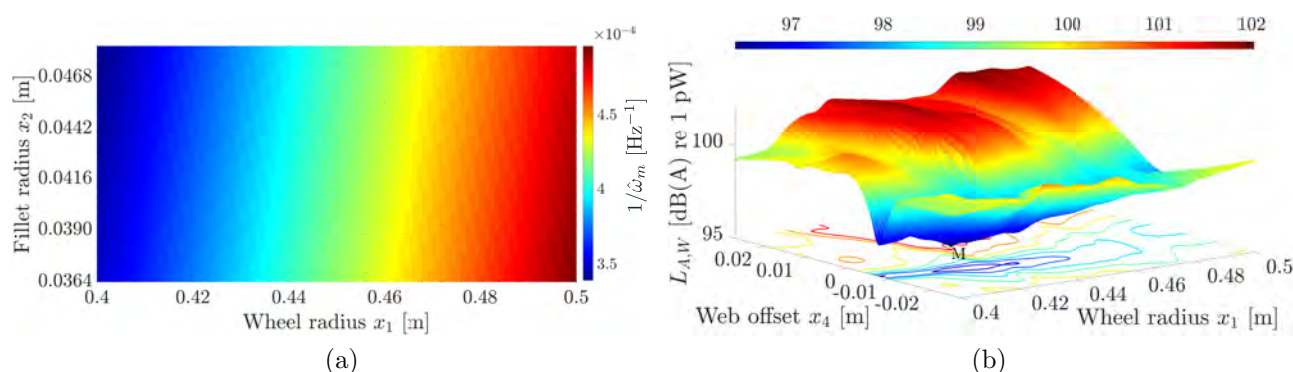


Figure 5: Response surfaces for different combinations of geometric parameters: (a) with Obj_{NF} for x_1 and x_2 ; (b) with $Obj_{L_{A,W}}$ for x_1 and x_4 . Fixed values correspond to those of the BFS for the corresponding optimization procedure and points M indicate the RS minima.

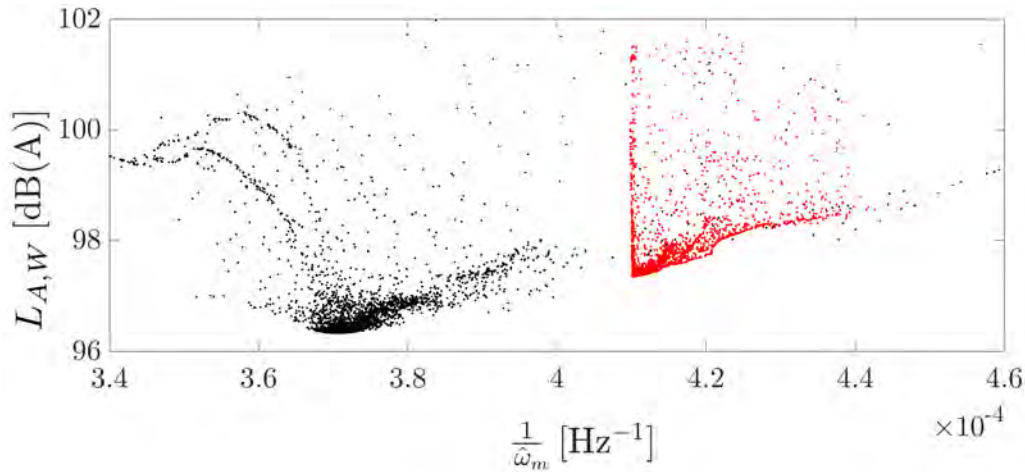


Figure 6: Obj_{NF} and $Obj_{L_{A,W}}$ values for candidate evaluations corresponding to the optimization runs using the $L_{A,W}$ -min methodology. Black points are evaluations in a run with a design space consisting of all x_1 to x_4 variables. Red points are evaluations in a run considering a fixed wheel radius variable x_1 .

each objective functions when modifying the wheel shape are established, identifying the radius x_1 and web offset x_4 as the principal factors in the changes observed. Finally, local correlations are found between the NF-max and $L_{A,W}$ -min objective functions behaviour, although not for the totality of sampled wheel cross-sections. In all cases, the observed patterns are related with the existence of design variables with significant influence on the acoustic performance although not in a noticeable way on the fixation of the natural frequencies.

6 ACKNOWLEDGEMENTS

This study has been supported by the Agencia Estatal de Investigación and the European Regional Development Fund (project TRA2017-84701-R).

7 REFERENCES

- [1] World Health Organization European Centre for Environment and Health, “Burden of disease from environmental noise,” WHO, Tech. Rep., 2011.
- [2] D. J. Thompson, *Railway Noise and Vibration. Mechanisms, modelling and means of control*, 1st ed. Elsevier, 2010. DOI: 10.1016/B978-0-08-045147-3.X0023-0.
- [3] D. J. Thompson, “Wheel-rail noise generation, part I: Introduction and interaction model,” *Journal of Sound and Vibration*, vol. 161, no. 3, pp. 387–400, 1993. DOI: 10.1006/jsvi.1993.1082.
- [4] J. Oertli, “The STAIRRS project, work package 1: A cost-effectiveness analysis of railway noise reduction on a European scale,” *Journal of Sound and Vibration*, vol. 267, no. 3, pp. 431–437, 2003. DOI: 10.1016/S0022-460X(03)00705-3.
- [5] D. J. Thompson, B. Hemsworth, and N. Vincent, “Experimental validation of the TWINS prediction program for rolling noise, part 1: Description of the model and method,” *Journal of Sound and Vibration*, vol. 193, no. 1, pp. 123–135, 1996. DOI: 10.1006/jsvi.1996.0252.
- [6] D. J. Thompson, “Wheel-rail noise generation, part II: Wheel vibration,” *Journal of Sound and Vibration*, vol. 161, no. 3, pp. 401–419, 1993. DOI: 10.1006/jsvi.1993.1083.

- [7] D. J. Thompson, “Wheel-rail noise generation, part IV: Contact zone and results,” *Journal of Sound and Vibration*, vol. 161, no. 3, pp. 447–466, 1993. DOI: 10.1006/jsvi.1993.1085.
- [8] F. Fahy and P. Gardonio, *Sound and Structural Vibration*, 2nd ed. Academic Press, 2007, ch. 3, pp. 135–241. DOI: 10.1016/B978-012373633-8/50007-7.
- [9] D. J. Thompson and C. J. C. Jones, “Sound radiation from a vibrating railway wheel,” *Journal of Sound and Vibration*, vol. 253, no. 2, pp. 401–419, 2002.
- [10] M. Petyt, *Vibration of Solids*, 2nd ed. Cambridge University Press, 2010. DOI: 10.1017/CB09780511761195.007.
- [11] J. C. O. Nielsen and C. R. Fredö, “Multi-disciplinary optimization of railway wheels,” *Journal of Sound and Vibration*, vol. 293, no. 3-5, pp. 510–521, 2006. DOI: 10.1016/j.jsv.2005.08.063.
- [12] UNE, “Railway applications. Wheelsets and bogies. Monobloc wheels. Technical approval procedure. Part 1: Forged and rolled wheels. UNE-EN-13979-1:2006,” Asociación Española de Normalización (UNE), Technical Standard, 2011.
- [13] X. Garcia-Andrés, J. Gutiérrez-Gil, J. Martínez-Casas, and F. D. Denia, “Wheel shape optimization approaches to reduce railway rolling noise,” *Structural and Multidisciplinary Optimization*, 2020. DOI: 10.1007/s00158-020-02700-6.